

Prediction of tensile capacity of single adhesive anchors using neural networks

Sherief S.S. Sakla^a, Ashraf F. Ashour^{b,*}

^a *Structural Engineering Department, Tanta University, Tanta, Egypt*

^b *EDT1, School of Engineering, Design and Technology, University of Bradford, Bradford BD7 1DP, W Yorkshire, UK*

Received 30 June 2004; accepted 16 February 2005

Available online 18 April 2005

Abstract

The tensile capacity of single adhesive anchors depends on many design parameters. Some of these parameters, such as chemical resin type, resin system and anchor bolt type are difficult to quantify in design models. Due to the complexity of developing rational models for estimating the tensile capacity of such type of anchors, most specifications recommend that the performance of these anchors be determined by product-specific and condition-specific testing. In this study, an attempt to predict the tensile capacity of single adhesive anchors using artificial neural networks (ANNs) is presented. A multilayered feed-forward neural network trained with the back-propagation algorithm is constructed using 7 design variables as network inputs and the uniform bond strength of adhesive anchors as the only output. The ANN was trained and verified using the comprehensive worldwide adhesive anchor database of actual tests compiled by the ACI Committee 355. Different modes of failure observed in experiments but bolt breakage are covered by the trained ANN.

The predictions obtained from the trained ANN showed that the tensile capacity of adhesive anchors is linearly proportional to the embedment depth as suggested by the uniform bond stress model. The effect of the concrete compressive strength on the tensile capacity of adhesive anchors is product dependent. The results indicate that ANNs are a useful technique for predicting the tensile capacity of adhesive anchors.

© 2005 Elsevier Ltd. All rights reserved.

Keywords: Adhesives; Anchors; Fasteners; Concrete; Embedment; Neural networks; Prediction; Capacity; Database

1. Introduction

Bonded anchors are increasingly employed as structural fastenings to hardened concrete. They can be clas-

sified as adhesive bonded or grouted anchors depending on the bonding agent, anchor type and hole diameter. An adhesive anchor is installed using a reinforcing bar or threaded rod inserted in a drilled hole in hardened concrete using a polymer-based bonding agent including epoxies, vinyl esters and polyesters. Typically, the drilled hole diameter is only about 10% to 25% larger than the anchor diameter. On the other hand, a grouted anchor is a threaded rod, headed bolt or deformed reinforcing bar inserted in a drilled hole filled with a cementitious

* Corresponding author. Tel.: +44 1274 233 870; fax: +44 1274 234 124.

E-mail addresses: sakla2000@softhome.net (S.S.S. Sakla), a.f.ashour@bradford.ac.uk (A.F. Ashour).

Nomenclature

d	outer diameter of fastener	t_k	actual response
d_0	hole diameter	u	net input signal of neurons
f'_c	cylinder compressive strength of concrete	w_j	synaptic weight of neuron j
$f(u)$	activation function	x_k	target output
h_{ef}	embedment depth of the anchor	α	performance ratio of weight-decay regularization
M	size of training data	β and γ	two constants required for concrete cone model
MSE	mean sum of squares of the network errors of the training set	λ	stiffness characteristic of the adhesive anchor system
MSE _{reg}	regularized error function	τ	bond strength
N	number of neuron in a layer		
N_u	tensile capacity of adhesive anchors		
r	coefficient of correlation		

or polymer grout. In this case, the diameter of the pre-drilled hole is at least 150% larger than that of the fastener.

Recently, more research has focused on adhesive bonded anchors [22,6,8,7,10]. Cook et al. [8] conducted a comprehensive investigation on previously published models for the design of single adhesive anchors subjected to tension loading in uncracked concrete. They concluded that the uniform bond stress model provides the best fit to a worldwide database of 888 tests. Cook and Konz [7] conducted a comprehensive test program investigating various factors influencing the bond strength of polymer-based adhesive anchors. The variables investigated included the condition of the drilled hole, concrete compressive strength, aggregate type, adhesive curing period and loading at elevated temperature. They recommended that reliable predictions of adhesive anchor performance are only practical by product-specific and condition-specific testing.

The last decade has witnessed an accelerated interest in the application of artificial neural networks to different civil engineering applications [3,11,12]. An artificial neural network (ANN) is an assembly of a large number of highly connected nodes. The ANN has the ability to learn by examples of past data and to generalise this knowledge by making predictions for previously unseen input data. The principal aim of this paper is to develop a multilayered feed-forward neural network trained with the back-propagation algorithm to model the complex nonlinear relationship between different parameters and the tensile capacity of adhesive anchors. The availability of a worldwide adhesive anchor database compiled by the ACI 355 is essential to train and validate the artificial neural network developed in this research. The trained neural network is then used to conduct a parametric study to establish the importance of different input parameters on the tensile capacity of those anchors.

2. Research significance

The large number of variables governing the behaviour of adhesive anchors has made it difficult to develop a generalised formula for the prediction of their tensile capacity. Current proposals for adhesive anchor design are based on using a uniform bond stress model where the value for the bond stress to be used in the model is determined by a comprehensive product evaluation test standard. The ACI 318-02 [1] included a new appendix, entitled “Appendix D—Anchoring to Concrete”, that provides provisions for computing the load-carrying capacity of both cast-in-place and post-installed anchors in either cracked or uncracked concrete. However, it does not include any provisions for estimating the load-carrying capacity of adhesive anchors. For failure mechanisms other than bolt breakage, such as partial or overall coning, the scatter of data is significant and therefore more difficult to put into a simple relationship. In addition, the large number of non-numeric parameters involved in the problem has suggested the use of artificial neural network modelling rather than other statistical regression analysis techniques. The advantage of using the neural network procedure presented in this paper is that the variables associated in establishing a bond stress value for a product could be directly built into the neural network model.

3. Current models for adhesive bonded anchors

3.1. Failure modes of adhesive-bonded anchors

Fig. 1 presents typical failure modes observed for adhesive anchors installed in hardened concrete [6,8,5,22,2]. For a very small embedment depth of an adhesive anchor, a concrete cone is usually pulled out as shown in Fig. 1a. When the embedment of the anchor is increased, a bond failure below a shallow concrete

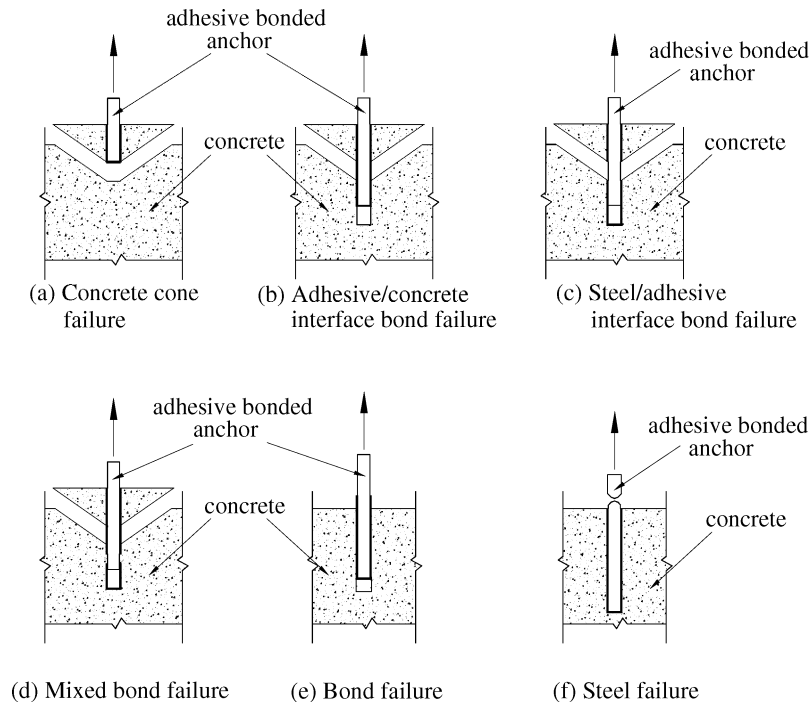


Fig. 1. Failure modes observed for adhesive anchors: (a) concrete cone failure; (b) adhesive/concrete interface bond failure; (c) steel adhesive interface bond failure; (d) mixed bond failure; (e) bond failure; (f) steel failure.

cone is observed. The bond failure can be at the adhesive/concrete interface (Fig. 1b), at the steel/adhesive interface (Fig. 1c), or a mixed bond failure (Fig. 1d) with failure at the adhesive/concrete and steel/adhesive interfaces in the upper and lower portions of the anchor, respectively. In some installations, bond failure without a concrete cone, as shown in Fig. 1e, may occur if the bonded surface lacks adequate strength due to the adhesive itself, improper curing, or inadequate hole preparation. If the embedment is very deep, the bond is so strong that the steel failure occurs in the anchor (Fig. 1f).

3.2. Tensile capacity of adhesive bonded anchors

Adhesive bonded anchors transfer loads by adhesion to the concrete along the entire embedment length of the anchor. Several design models [6,8] for adhesive anchors have been proposed and are summarized below:

1. *Concrete cone models*: models that are dependant on the square root of the concrete compressive strength and the embedment length raised to a power (no influence of anchor diameter).
2. *Bond models*: models that are dependant on the bond strength of the product, the diameter, and the embedment length.
3. *Bond models neglecting the shallow concrete cone*: similar to bond models except that the embedment length is reduced to account for the shallow concrete cone.
4. *Cone models with bond models*: models that use concrete cone formulas for shallow embedments and bond stress formulas for deeper embedments.
5. *Combined cone/bond models*: models that use concrete cone formulas for shallow embedments and combined cone/bond models for deeper embedments.
6. *Two interface bond model*: bond models that are based on distinguishing between bond failure modes at the steel/adhesive interface and adhesive/concrete interface.

Cook et al. [8] carried out comparisons between various design models for single adhesive anchors and a worldwide database of adhesive anchor tests. They concluded that the model based on uniform bond stresses provides a better fit to the database than other more complicated design models. They highly recommended using the uniform bond stress model to estimate the adhesive anchor capacity with an optional modification factor to account for concrete strength. These conclusions were supported by the non-linear analytical work of McVay et al. [19]. The bond stress models are mainly

dependent on the bond strength between the steel/adhesive interface or the concrete/adhesive interface. Cook and Konz [7] demonstrated that the bond strength is product and condition dependent and must be determined experimentally. The basic uniform bond stress model (Cook et al. [8]) is given by:

$$N_u = \pi \tau d_o h_{ef} \quad (1)$$

where N_u —the tensile capacity of adhesive anchors; τ —the uniform bond strength; d_o —the hole diameter; and h_{ef} —the embedment depth of the anchor.

4. Artificial neural network background

Artificial neural network (ANN) models are composed of a large number of simple processing units known as neurons that are organized in layers and are connected to each other to form a network of dense connections. The connections have weights associated with them referred to as synaptic weights. Each signal travelling along a connection is multiplied by the connection weight. A neural network accepts certain inputs and produces certain outputs. The computing power of an ANN is derived through its massively parallel-distributed structure and its ability to learn and generalize. A detailed description of the basic anatomy of different types of neural networks is beyond the scope of this paper and can be found in the literature [20,16,15]. The principles and applications of ANNs in civil engineering are summarized in the work by Flood and Kartam [11,12] and Adeli [3].

The functionality of a neural network depends on its structure and on the model of each neuron in that structure. The most widely used neuron model is based on McCulloch and Pitts' work [18] and is illustrated in Fig. 2. In ANNs, a neuron can have multiple input signals, N , originating from neurons in a previous layer but it sends only one output signal. Each neuron model consists of two parts: the net function and the activation function. The net function determines how the input signals coming from neurons in a previous layer, $\{y_j; 1 \leq j \leq N\}$, are combined together to form the net input

signal inside the neuron. The net input signal, u , of this kind of neurons may be expressed by the weighted sum of all its input signals:

$$u = \sum_{j=1}^N w_j y_j + \theta \quad (2)$$

where $\{w_j; 1 \leq j \leq N\}$ are the synaptic weights converging to a neuron. The quantity θ is called the bias and is used to model the threshold. The output signal of the neuron, denoted by a in Fig. 2, is related to the network input u via a transformation function called the activation function.

$$a = f(u) \quad (3)$$

In various ANN models, different activation functions have been proposed. The sigmoid activation function, given by Eq. (4), is one of the most common forms of an activation function used in the construction of ANNs. This function performs a smooth mapping $(-\infty, +\infty)$ to $(0, 1)$.

$$f(u) = \frac{1}{1 + e^{-u}} \quad (4)$$

The class of ANNs used in this paper is referred to as multilayered feed-forward neural networks. This type of ANNs is one of the best-developed and most widely used neural networks. In this type of ANNs, the data flows in one direction from the input layer to the output layer, i.e. no feedback loop presents. Fig. 3 shows the architecture of the one-hidden-layer, one output variable feed-forward ANN used in this study. The first layer is the input layer where the input neurons distribute the inputs to neurons in subsequent layers. No calculations are performed in the input nodes. The output layer represents the output of the ANN. The layer sandwiched between the input and output layers is called hidden layer.

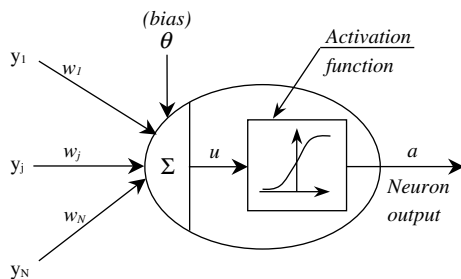


Fig. 2. McCulloch and Pitts neuron model.

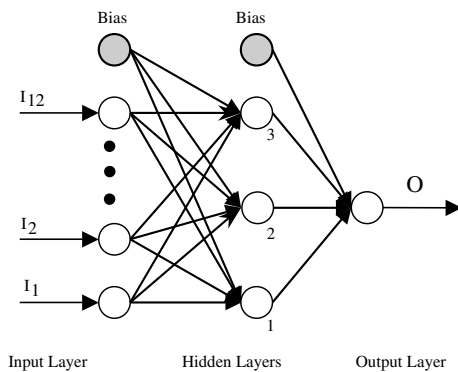


Fig. 3. A schematic diagram of typical neural network architecture.

5. Experimental data

A large quantity of experimental research has been conducted on adhesive bonded anchors in concrete to fully understand their behaviour. In order to establish a universal design approach of adhesive anchors, the ACI Committee 355 collected all worldwide relevant test data of adhesive bonded anchors and compiled them into a database system. From 38 reports and papers published in Europe, USA and Japan, the results of 2929 tests have been included in the database system [8]. This comprehensive worldwide adhesive anchor database is used to provide the experimental data needed to train and validate the proposed ANN.

The database contains tensile and shear load testing of single anchors, groups of two and four anchors in uncracked and cracked concrete. It distinguishes between confined and unconfined tests as well as tests far from the concrete edge, tests near the concrete edge and tests with close anchor spacing. The database also includes tests of different types of anchors; such as threaded rods, insert sleeves and rebars bonded with epoxies, vinyl esters, unsaturated polyesters, hybrid adhesives, inorganic adhesive and grout. The database is maintained by Professor R. Cook at the University of Florida.

For the purpose of this study, only test results satisfying the following criteria are selected:

- Single anchor tests or where the minimum spacing between anchors in a group was greater than 1.6 of the embedment depth.
- Anchors located away from the concrete edge by a distance greater than 0.80 of the embedment depth.
- Tests carried out in uncracked and unconfined concrete; tests of anchors conducted in cracked or confined concrete are not included.
- Anchors tested under short term tensile static loads; those tested under shear loads are not studied.
- Anchors inserted in cleaned and dried holes; tests carried out on anchors inserted in uncleaned wet holes are excluded. It is a common practice to clean the drilled holes before the insertion of the anchors.
- Only tests carried out at room temperature were considered (i.e. at an air and base material temperatures range of 13–30 °C). Tests carried out at temperatures out of this range were excluded.
- Anchors that failed due to bolt breakage are excluded as a reliable design equation exists for the prediction of this mode of failure.

Considering only those tests that satisfy the above-mentioned criteria resulted in a reduced database with a total of 1143 data entries covering all possible mechanisms of failure except for bolt breakage. Factors affecting the tensile capacity of single adhesive anchors such

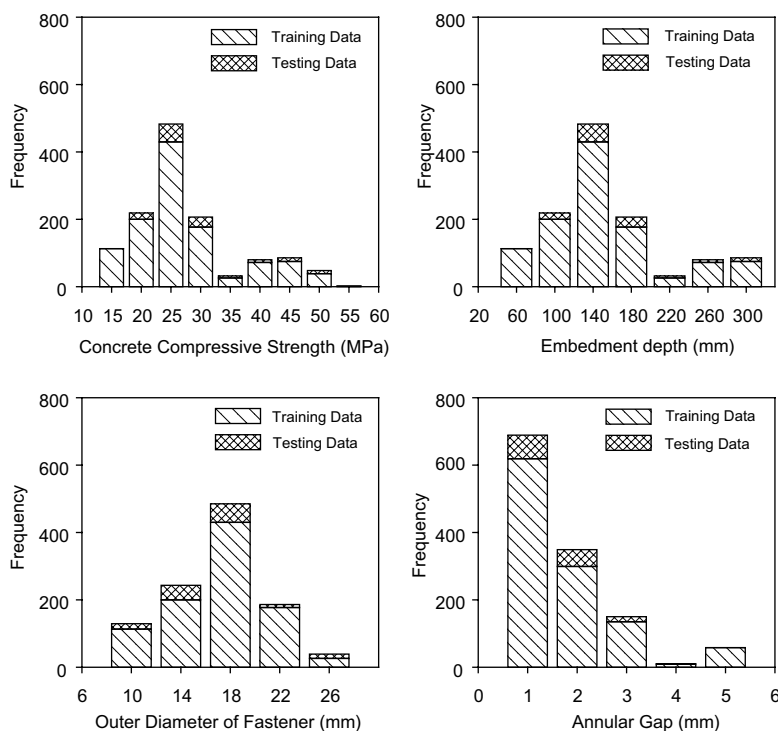


Fig. 4. Distribution of different numeric design variables in the reduced database.

Table 1
Distribution of non-numeric design variables in the reduced database

Design variable	Number of tests	
	All data	Testing data set
<i>Chemical resin type</i>		
Epoxy	184	31
Vinylester	670	84
Hybrid mortar	289	19
<i>Anchor bolt type</i>		
Threaded rod	834	106
Reinforcing bar	202	18
Internal threaded sleeve	107	10
<i>Grout/injection type</i>		
Glass capsule	266	18
Cartridge injection anchor system	877	116

as the edge distance, anchor spacing, temperature, cleaning condition of the hole and cracked concrete were not included in this study as design variables as they were under-represented in the worldwide database. The distribution of different numeric design variables in the reduced database used for training and testing the developed ANN is presented as histograms in Fig. 4 and that of different non-numeric design variables is given in Table 1.

6. Training and validation of the neural network

A multilayered feed-forward neural network with a back-propagation algorithm was adopted in this study. The ANN was developed using the popular MATLAB software package [21] and its neural network toolbox [9]. This ANN consisted of an input layer, a single hidden layer and an output layer. The inputs of the neural network consisted of the following variables affecting the capacity of adhesive anchors:

1. The cylinder compressive strength of concrete, f'_c .
2. Anchor embedment depth, h_{ef} .
3. Outer diameter of fastener, d .
4. Drilled hole clearance (the difference between the radius of the drill bit and anchor).
5. Chemical resin type (epoxy, vinylester, or hybrid mortar).
6. Anchor bolt type (threaded rod, reinforcing bar, or internal threaded sleeve).
7. Grout/injection system (glass capsule or cartridge injection anchor system).

Ranges of different input parameters are given in Table 2. Each of the first four numeric design variables

Table 2
Ranges of input parameters in database

Net input parameters	Range	
	Minimum	Maximum
Cylinder compressive strength of concrete (MPa)	13.37	55.25
Anchor bolt embedment depth (mm)	76.2	320.0
Outer diameter of fastener (mm)	8.0	25.4
Drilled hole clearance (mm)	0.5	5.0
Chemical resin type	Epoxy Vinylester or Hybrid mortar	
Anchor bolt type	Threaded rod Reinforcing bar or Internal threaded sleeve	
Grout/injection type	Glass capsule or Cartridge injection anchor system	

was represented by a single quantitative neuron in the input layer. All of numeric variables were normalized to a range of [0,1] before being introduced to the ANN using the values listed in Table 2 and the following equation:

$$I_n = \frac{I - I_{\min}}{I_{\max} - I_{\min}} \quad (5)$$

where I_n and I are the normalized and unnormalized values of the training set, I_{\max} and I_{\min} are the maximum and minimum values of the data set under normalization, respectively. Normalization of the input data greatly improves the learning speed and is beneficial in reducing the error of the trained network [21]. Each of the remaining three non-numeric design variables was represented by qualitative neurons taking values of either 0 or 1. For example, the chemical resin type was represented by three qualitative neurons, each for a chemical resin type (epoxy; vinylester or hybrid mortar). If epoxy was used, the epoxy neuron was assigned a value of one and both the vinylester and hybrid mortar neurons were assigned a value of 0. A similar approach was used for the anchor bolt type and grout/injection system. Following this approach, the input layer consisted of four quantitative neurons and 8 qualitative neurons. In any single run, only 7 neurons are active.

The only neuron of the neural network output layer produced the equivalent uniform bond strength, where the equivalent uniform bond strength is the normalized tensile capacity by the embedded surface area of the anchor, $\pi d h_{ef}$. The normalized bond strength of the reduced database ranged from 3.4 to 22.4 MPa.

To train the ANN model, first the entire training data file was randomly shuffled and divided into training and testing data sets as shown in Fig. 4 and Table 1. After extracting the testing data set from the database, the remaining training data set was examined to make sure that ranges of different input parameters shown in Table 1 and Fig. 4 are still covered by the training data set. 88% of the data, 1009 patterns, was used to train the network while the remaining 12%, 134 data patterns, was employed for testing the developed network. It should be mentioned that, during the dividing of the reduced database into training and testing data sets, attention was paid to ensure that database entries with identical input parameters (i.e. repeated tests representing the same case) were entirely present in either the training or the testing data set. As could be shown from Fig. 4 and Table 1, the testing data set is representative of the population of the available database and contains all of the patterns that are present in that database.

7. Network training and regularization technique

An ANN with a sufficient number of neurons can be trained to map any input-output relationships [3,4,15]. During the training process of a feed-forward ANN, all network weights and biases are adjusted using an iterative back-propagation procedure until the discrepancy between the target output, x_k , and the actual response, t_k , is minimized. The performance function is normally chosen to be the mean sum of squares of the network errors of the training set (MSE).

$$MSE = \frac{1}{M} \sum_{k=1}^M (x_k - t_k)^2 \quad (6)$$

where M is the size of training data. This type of error function is continuous and differentiable, so it can be used in gradient based optimization techniques such as steepest descent, quasi-Newton or Levenberg–Marquardt methods [4,15]. After successful training, the network weights and biases are fixed and used for prediction purposes.

There are three ways to get better generalization performance for a given size of training set. The first is to reduce the number of adjustable weights, e.g. by reducing the number of hidden units; the second way is to use early stopping which requires a validation set; and the third way is to use weight-decay regularization. Weight-decay regularization involves modifying the performance function by adding a term that involves the sum of squares of the network weights and biases to improve the generalization capabilities of the trained ANN. The addition of this term to the performance function forces the network to have smaller weights and biases and this results in a smoother network response that is not likely to overfit.

In this study, the weight and bias values were updated according to the Levenberg–Marquardt optimization [14]. The regularized error function, MSE_{reg} , to be minimized is a combination of MSE and the mean sum of squared weights and biases, MSW:

$$MSE_{reg} = \alpha(MSE) + (1 - \alpha)(MSW) \quad (7)$$

where α is the performance ratio. The difficulty with regularization is in assigning an optimum value for the performance ratio, α . If the performance ratio parameter is selected too large, this may cause over-fitting. On the other hand, if it is too small, the network will not adequately fit the training data. Therefore, it is desirable to determine the optimal regularization parameters in an automated fashion. In this study, the optimum performance ratio was determined by a Bayesian approach [17]. In this approach the weights and biases of the network are assumed to be random variables with specified distributions. The regularization parameters are related to the unknown variances associated with these distributions. Statistical techniques can then be used to estimate these parameters. A detailed discussion of the use of Bayesian regularization, in combination with Levenberg–Marquardt training, can be found in the work by Foresee and Hagan [13].

The initial values of the weights and biases are randomly chosen from a normal distribution with mean zero and variance one. The training is repeated twenty times with different initializations; the parameters of the network which exhibit the best performance were taken as the final parameters of the ANN.

8. Architecture of hidden layers

So far, there is no rule for estimating the optimal number of hidden layers and number of nodes in each hidden layer, except through experimentation. The number of hidden nodes in an ANN should be sufficient to approximate the function relating the input variables and the output but, in the mean time, should be restricted in order to avoid overfitting of the training data and to allow interpreting the results of the trained ANN in a physical sense. For the current application, overfitting is not a concern due to the use of Bayesian regularization but for the sake of interpreting the results an ANN with the smallest number of hidden nodes should be used. A network with a single hidden layer was initially tried. The number of neurons assigned to the single hidden layer was increased from one to seven neurons. Experimentation with the utilization of the sigmoid activation function, Eq. (4), revealed that a lowest prediction error of a certain network configuration is obtained if no activation function was applied at the output neuron. As a result, it was decided to use the sigmoid activation function at the hidden layer only. The

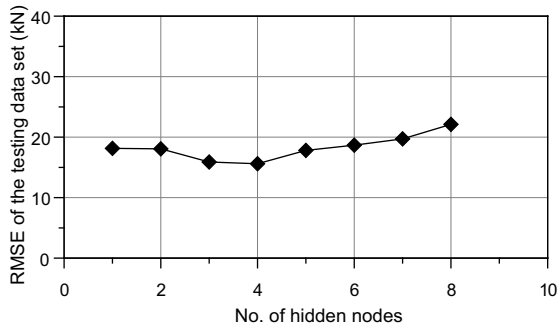


Fig. 5. Effect of changing the number of nodes in the hidden layer on the performance of the ANN model.

effect of changing the number of hidden neurons on the root-mean-square-error (RMSE) of the testing data set is shown in Fig. 5. It could be shown that the effect of the number of neurons assigned to the hidden layer has a little effect on the performance of the ANN model. As could be concluded from Fig. 5, the use of three or four neurons gives the lowest prediction error in the testing data set. However, in order to keep the ANN as simple as possible, it was decided to use a single hidden layer of three neurons. The RMSE of this network is 15.88 kN, as shown in Fig. 5, which is not far from that of the network with 4 hidden neurons. Fig. 5 shows that a network with simple structure (i.e. small number of weights) were capable of simulating the training and testing data. Increasing the number of hidden layers would definitely increase the capacity of the network which is not a benefit for the case at hand. Therefore, it was decided to use a single hidden layer of three neurons in this study.

9. Performance of the developed neural network

A comparison between the experimental and predicted values of the tensile capacity of anchor bolts is shown in Figs. 6 and 7 for the training and testing data sets, respectively. As could be concluded from these figures, the ANN was successful in learning the relationship between the input and output data. High coefficients of correlation and low mean absolute errors were obtained for both training and testing data sets. The coefficient of correlation, r^2 , was 0.935 and 0.941 for the training and testing data sets, respectively. The average ratio of actual capacity to predicted capacity of the training and testing data sets is 1.00 and 1.03, respectively. The mean absolute percentage of error is 16.8% and 14.1% for the training and testing data sets, respectively. This mean absolute error is fairly reasonable considering the noisy nature of the experimental results of adhesive anchors in the database. A careful

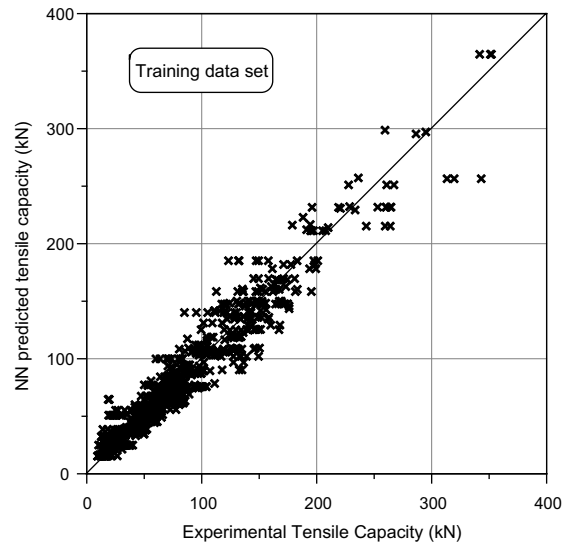


Fig. 6. Comparison of experimental and predicted ultimate tensile capacities for the ANN training data set.

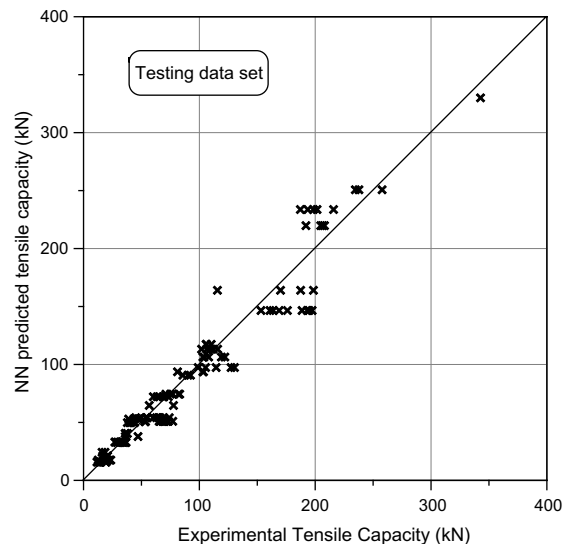


Fig. 7. Comparison of experimental and predicted ultimate tensile capacities for the ANN testing data set.

inspection of the experimental database reveals that there exists considerable variation among results representing replicate tests of a certain anchor reported by the same source and tested under identical conditions. In some instances, a coefficient of variation in a group of replicate tests exceeding 0.30 was recorded.

Fig. 7 shows that the ANN model is capable of predicting, with a certain degree of accuracy, the ultimate tensile capacity of the 134 testing patterns although these data patterns were not used for training of the

ANN which implies that the trained ANN is capable of generalization.

10. Parametric study and comparisons with other models

To further test its generalization capability, the ANN was used to conduct a parametric study to investigate the effects of different input parameters on the tensile capacity of adhesive anchor bolts.

10.1. Effect of concrete compressive strength and chemical type

Fig. 8 shows the effect of changing the compressive strength of concrete on the ultimate tensile load-carrying capacity of threaded anchor bolts for different chemi-

cal adhesive types. Three different bolt sizes were used: the first bolt was 24 mm diameter and 200 mm embedment depth; the second bolt was 16 mm diameter and 125 mm embedment depth; while the third bolt was 8 mm diameter and 80 mm embedment depth, as shown in Fig. 8a–c, respectively. The annular gap was taken equal to 1.5 mm, 1 mm, and 1 mm for the 24 mm diameter, 16 mm diameter, and 8 mm diameter anchor bolts, respectively. The compressive strength of concrete was varied from 15 to 45 MPa in increments of 5 MPa. Fig. 8 indicates that epoxy-based adhesives outperform ester-based adhesives as concluded by Cook and Konz [7]. Regression analysis of the curves shown in Fig. 8 revealed that the tensile capacity is almost linearly proportional to the compressive strength, contrary to that suggested by the concrete cone model.

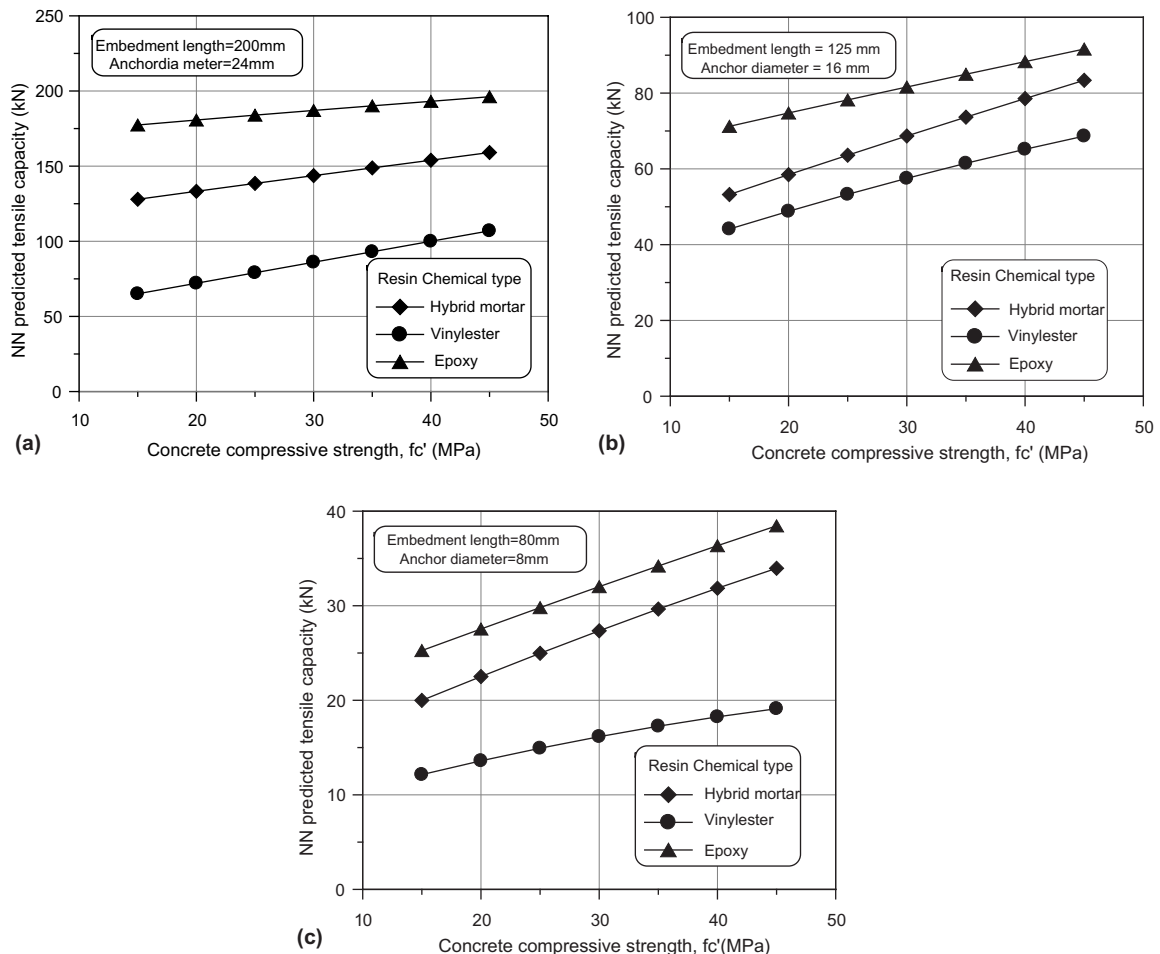


Fig. 8. Effect of concrete compressive strength on the predicted ultimate tensile capacity: (a) embedment depth h_{ef} = 200 mm and anchor diameter = 24 mm; (b) embedment depth h_{ef} = 125 mm and anchor diameter = 16 mm; (c) embedment depth h_{ef} = 80 mm and anchor diameter = 8 mm.

10.2. Effect of embedment depth and bolt type

The embedment depth is one of the most significant factors that affect the ultimate tensile capacity of adhesive anchor bolts. A 16 mm-diameter anchor bolt installed using glass-capsule epoxy-based adhesive was considered for the purpose of studying the effect of the embedment depth. The compressive strength of concrete is 25 MPa and the annular gap of the hole is 1 mm. Fig. 9 shows the effect of changing the embedment depth on the ultimate tensile capacity of adhesive anchor bolts for different types of bolts.

As could be noted from Fig. 9, rebar anchor bolts slightly outperform sleeve and threaded anchor bolts. In general, increasing the embedment depth of adhesive anchor bolts resulted in a near-linear increase in the tensile load-carrying capacity, agreeing more with the uniform bond stress model than the concrete cone model.

10.3. Effect of anchor diameter

Fig. 10 shows the effect of increasing the anchor bolt diameter on the predicted ultimate tensile capacity for different chemical adhesive types. A threaded anchor bolt of 160 mm embedment depth inserted using cartridge injection was used for this purpose. The compressive strength of concrete is 25 MPa and the annular gap of the hole is 10% of the anchor diameter. As observed in Fig. 10, the increase of anchor diameter caused a linear increase in the tensile capacity of the adhesive anchor inserted using epoxy-based adhesive agreeing well with the bond stress models of adhesive anchors. For ester-based and hybrid mortar, the increase in the tensile capacity was initially linear up to anchor diameter of 12 mm and then the rate of increase of the tensile capacity was reduced. Fig. 10 confirms the conclusion that

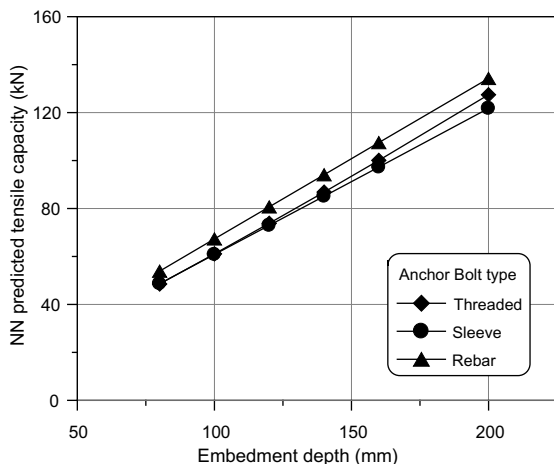


Fig. 9. Effect of the anchor bolt type and the embedment length on the predicted ultimate tensile capacity.

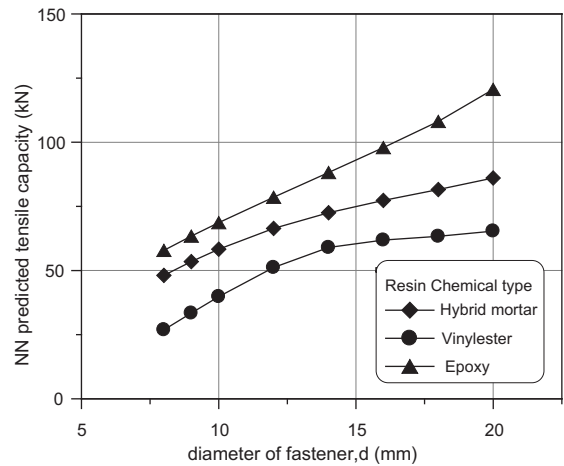


Fig. 10. Effect of the anchor bolt diameter on the predicted tensile bond strength.

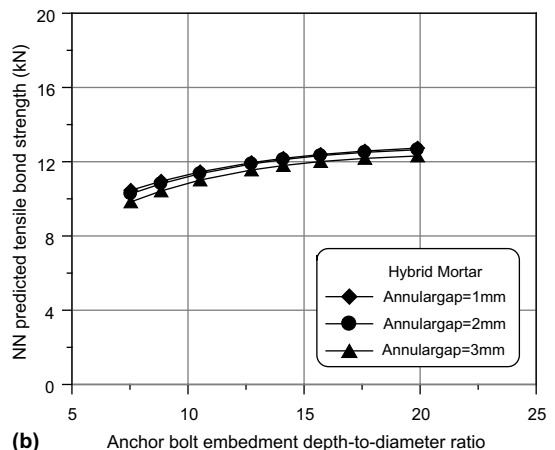
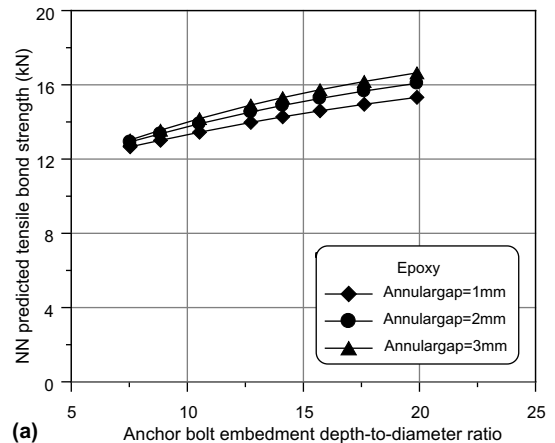


Fig. 11. Effect of the anchor bolt embedment depth-to-diameter ratio on the predicted tensile bond strength: (a) epoxy-based adhesive; (b) hybrid mortar adhesive.

epoxy-based adhesives outperform hybrid-mortar adhesives which, in turn, outperform ester-based adhesives.

10.4. Effect of anchor embedment length-to-diameter ratio and annular gap

Fig. 11 shows the effect of increasing the anchor bolt embedment depth-to-diameter ratio on the predicted uniform bond strength for three different annular gap values. A threaded anchor bolt with a surface area of 4000 mm² inserted using cartridge-injection epoxy-based adhesive and Hybrid mortar was used for the purpose of studying the effect of the anchor embedment length-to-diameter ratio. The compressive strength of concrete is 25 MPa and the annular gap of the hole was taken as 1, 2 and 3 mm.

As observed in Fig. 11, the thickness of the annular gap has an insignificant effect on the uniform bond strength of adhesive anchor bolts inserted using epoxy-based adhesives or hybrid mortar. The rate of uniform bond strength gain is reduced with the increase of anchor embedment depth-to-diameter ratio. This could be attributed to the formation of a shallow concrete cone of a fixed depth at the upper portion of the anchor as observed in experiments (see Fig. 1b–d). As the depth of this cone is independent on the embedment depth of the anchor, its detrimental effect on the predicted uniform bond strength becomes less as the anchor embedment length increases.

11. Conclusions

A back-propagation neural network with Levenberg–Marquardt training algorithm and Bayesian regularization was successfully trained to predict the ultimate tensile capacity of single anchor bolts in uncracked concrete. The training of the ANN was achieved using experimental data extracted from the comprehensive worldwide adhesive anchor database collected by ACI Committee 355. High coefficients of correlation and low mean absolute errors were obtained for both training and testing sets of data indicating that the ANN has learned to map the relationship between the ultimate tensile capacity of single anchor bolts and the influencing parameters. The developed ANN and observations from the parametric study given in this paper are valid for the limits of the database shown in Table 2. As more tests on adhesive anchors will be available, the ANN could be re-trained and its range of applicability could be extended.

Based on the parametric study conducted using the trained ANN, the following conclusions may be drawn:

- The tensile capacity of adhesive anchors is linearly proportional to the anchor diameter and the embedment depth.

- Epoxy-based adhesives outperform hybrid-mortar adhesives that, in turn, outperform ester-based adhesives.
- The influence of the concrete compressive strength on the tensile capacity of the adhesive anchors is almost linear and depends on the chemical resin type.
- Overall, the uniform bond stress model is the most suitable one among those available in the literature for predicting the effect of different parameters on the tensile capacity of adhesive anchors.

Acknowledgement

The authors are grateful to Professor R. Cook for providing the database of adhesive bonded anchors. Professor Cook maintains this database on behalf of the ACI Committee 355.

References

- [1] ACI 318-02. Building code requirements for structural concrete (ACI 318-02) and Commentary (ACI 318R-02) American Concrete Institute, Detroit, USA, 2002.
- [2] ACI Committee 355 (1991). State-of-the-art report on Anchorage to concrete. American Concrete Institute, Detroit, USA, Re-approved 1997.
- [3] Adeli H. Neural networks in civil engineering: 1989–2000. *Comput-Aided Civil Inf Engng* 2001;16(2):126–142.
- [4] Bishop C. Neural networks for pattern recognition. Hhkjhk: Oxford University Press; 1996.
- [5] Comite Euro-International du Beton (CEB), Task Group VI/5. Fastenings to concrete and masonry structures. Thomas Telford Services Ltd, London, UK, 1994. p. 249.
- [6] Cook RA. Behaviour of chemically bonded anchors. *J Struct Eng* 1993;119(9):2744–62.
- [7] Cook RA, Konz RC. Factors influencing bond strength of adhesive anchors. *ACI Struct J* 2001;98(1):76–86.
- [8] Cook RA, Kunz J, Fuchs W, Konz RC. Behavior and design of single adhesive anchors under tensile load in uncracked concrete. *ACI Struct J* 1998;95(1):9–26.
- [9] Demuth H, Beale M. Neural Network Toolbox. Version 3, for use with MatLab, Mathworks Inc, 1998.
- [10] Eligehausen R, editor. Connections between steel and concrete, RILEM International Symposium, Pro. No. 21, Stuttgart, Germany, 2001. p. 1448 (2 Vol. Set).
- [11] Flood I, Kartam N. Neural networks in civil engineering. I: Principles and understanding. *J Comput Civil Eng* 1994; 8(2):131–48.
- [12] Flood I, Kartam N. Neural networks in civil engineering. II: Systems and applications. *J Comput Civil Eng* 1994; 8(2):149–62.
- [13] Foresee FD, Hagan MT. Gauss–Newton approximation to Bayesian regularization. *Proceedings of the IEEE Interna-*

- tional Conference on Neural Networks (ICNN'97), Houston, Texas, vol. 3; 1997. p. 1930–35.
- [14] Hagan MT, Menhaj M. Training feed forward networks with the Marquardt algorithm. *IEEE Trans Neural Networks* 1994;5(6):989–93.
- [15] Hagan MT, Demuth HB, Beale MH. *Neural network design*. Boston, MA: PWS Publishing Company; 1996.
- [16] Hertz J, Krogh A, Palmer RG. *Introduction to the theory of neural computing*. Calif: Addison Wisely; 1991.
- [17] MacKay DJC. Bayesian interpolation. *Neural Computation* 1992;4(3):415–47.
- [18] McCulloch WS, Pitts W. A logical calculus of the ideas immanent in nervous system. *Bull Math Biophys* 1943;5: 115–33.
- [19] McVay MC, Cook RA, Krishnamurthy K. Pullout simulation of post-installed chemically-bonded anchors. *J Struct Engng* 1996;122(9):1016–24.
- [20] Rumelhart DE, Hinton GE, Williams RJ. Learning internal representation by error propagation. In: Rumelhart DE, McClelland JL, editors. *Parallel distributed processing*, vol. 1. Cambridge, Mass.: MIT Press; 1986. p. 318–62.
- [21] The MathWorks Inc. *MatLab the language of technical computing*, Version 5.3, Natick, MA, 1999.
- [22] Zavliaris KD. *Mechanical behaviour of adhesive anchors installed in concrete*. PhD thesis, City University, UK, 1990.